THE JOURNAL OF BIOLOGICAL CHEMISTRY VOL. 284, NO. 19, pp. 12845–12852, May 8, 2009

Propagation of Tau Misfolding from the Outside to the Inside of a Cell*

Received for publication, November 19, 2008, and in revised form, March 2, 2009 Published, JBC Papers in Press, March 11, 2009, DOI 10.1074/jbc.M808759200

Bess Frost[‡§], **Rachel L. Jacks**[‡§], **and Marc I. Diamond**[‡§¶1]

From the Departments of [‡]*Neurology and* [¶]*Cellular and Molecular Pharmacology and* [§]*Biomedical Sciences Program, University of California, San Francisco, California 94143*

Tauopathies are neurodegenerative diseases characterized by aggregation of the microtubule-associated protein Tau in neurons and glia. Although Tau is normally considered an intracellular protein, Tau aggregates are observed in the extracellular space, and Tau peptide is readily detected in the cerebrospinal fluid of patients. Tau aggregation occurs in many diseases, including Alzheimer disease and frontotemporal dementia. Tau pathology begins in discrete, disease-specific regions but eventually involves much larger areas of the brain. It is unknown how this propagation of Tau misfolding occurs. We hypothesize that extracellular Tau aggregates can transmit a misfolded state from the outside to the inside of a cell, similar to prions. Here we show that extracellular Tau aggregates, but not monomer, are taken up by cultured cells. Internalized Tau aggregates displace tubulin, co-localize with dextran, a marker of fluid-phase endocytosis, and induce fibrillization of intracellular full-length Tau. These intracellular fibrils are competent to seed fibril formation of recombinant Tau monomer *in vitro*. Finally, we observed that newly aggregated intracellular Tau transfers between co-cultured cells. Our data indicate that Tau aggregates can propagate a fibrillar, misfolded state from the outside to the inside of a cell. This may have important implications for understanding how protein misfolding spreads through the brains of tauopathy patients, and it is potentially relevant to myriad neurodegenerative diseases associated with protein misfolding.

Tau filament deposition in Alzheimer disease (AD),[2] frontotemporal dementia (FTD), and other tauopathies correlates closely with cognitive dysfunction and cell death (1). Mutations in the *tau* gene cause autosomal dominant tauopathy, implicating Tau as the proximal cause (2–4). Specific disease phenotypes are defined by the early sites of pathology. For example, AD is characterized by memory loss that derives from involvement of hippocampal neurons, whereas FTD is characterized by personality changes that result from frontal lobe involvement (5). Pathology ultimately spreads to involve much larger regions of brain. Studies on patients with AD show a progressive, stereotyped spread of Tau deposits from the transentorhinal cortex to the hippocampus, and eventually to most cortical areas (6–8). Others have correlated the distribution of neurofibrillary tangles of Tau in AD brains with trans-synaptic distance from the affected areas (9). A similar spread affecting different subsets of neurons has been observed in other sporadic tauopathies, such as progressive supranuclear palsy (10). It is unknown why Tau misfolding progresses through the brain, whether it is a sequence of cell autonomous processes or whether a toxic factor is involved. Loss of synaptic connections and cell death may expose healthy cells to toxic factors and decrease available neurotrophins (11, 12). Another possibility is that the Tau protein itself serves as the agent of trans-cellular propagation. For example, it has been shown that extracellular Tau is toxic to cultured neuronal cells (13, 14). This is consistent with the observation that immunotherapy against Tau reduces pathology in a mouse model (15).

Tau is well known as an intracellular protein that stabilizes microtubule filaments (16); however, it is readily detected in cerebrospinal fluid (17) and as extracellular aggregates, termed "ghost tangles," in diseased brain. These are comprised predominantly of the microtubule-binding region (MTBR), the functional and pathogenic core of the Tau protein (18). We hypothesize that Tau aggregates present in the extracellular space enter naive cells and induce misfolding of intracellular Tau. We have tested this idea using cellular studies, biochemistry, and atomic force microscopy (AFM).

EXPERIMENTAL PROCEDURES

Tau Expression, Purification, and Fibrillization—The MTBR (amino acids 243–375) of full-length (P10636-8) wild-type *tau* (a gift from Dr. Virginia Lee) was subcloned into pRK172. HA-tagged MTBR Tau contains the sequence YPYDVPDYA on its C terminus. Recombinant Tau MTBR was prepared as described previously from Rosetta (DE3)pLacI competent cells (Novagen), exploiting the heat stability of Tau protein followed by cation exchange chromatography (19). Single-use aliquots were stored at −80 °C in 10 mM HEPES and 100 mM NaCl (pH 7.4). To induce fibrillization of Tau monomer, the MTBR was incubated at room temperature without agitation in 5 mM dithiothreitol, 10 mM HEPES (pH 7.4), 100 mM NaCl, and 150 μM arachidonic acid (Sigma). Incubation times from 3 to 24 h produced similar results.

* This work was supported, in whole or in part, by National Institutes of Health Grant R01 NS50284-03 from NINDS (to M. I. D.) and a National Institutes of Health grant from NINDS (training grant to B. F.). This work was also supported by grants from the Sandler Family Supporting Foundation, the Taube Family Foundation Program in Huntington Disease Research, and the Muscular Dystrophy Association.

[1] To whom correspondence should be addressed: GH-S572B 600 16th St., San Francisco, CA 94143-2280. Tel.: 415-514-3646; Fax: 415-514-4112; E-mail: marc.diamond@ucsf.edu.

[2] The abbreviations used are: AD, Alzheimer disease; AF488, AlexaFluor488; Tau-YFP, full-length Tau tagged with YFP; MTBR-YFP, microtubule-binding region tagged with YFP; FTD, frontotemporal dementia; AFM, atomic force microscopy; MTBR, microtubule-binding region; HA, hemagglutinin; PBS, phosphate-buffered saline.

Atomic Force Microscopy and Antibody Decoration—Tau fibrillization reactions were incubated on freshly cleaved mica (Ted Pella, Inc.) for 2 min. The sample was then rinsed twice with 200 μl of water. After washing, samples exposed to antibody decoration were incubated with 20 μg/ml Tau5 antibody (BD Biosciences) for 2 min. The sample was rinsed twice with water and left to dry for at least 1 h prior to tapping mode atomic force microscopy (Digital Instruments).

Western Blots—HEK293 or C17.2 cells were seeded 300,000 or 75,000 cells/well, respectively, in a 24-well plate. The following day, cells were transfected with 1.2 μg of full-length wild-type Tau-YFP or MTBR-YFP using Lipofectamine2000 (Invitrogen) according to the manufacturer's recommendations. After 15 h, cells were replated 1:4 in a 24-well plate, allowed to re-adhere for 5 h, and treated with 0.4 μM Tau buffer, monomer, or aggregates. After 15 h, cells were harvested with 0.25% trypsin for 3 min, pelleted, and lysed in 40 μl of 1% Triton in PBS plus a protease inhibitor tablet (Roche Applied Science) (lysis buffer). As an additional control, untreated cells were treated with an equivalent concentration of aggregates after lysis. Soluble and insoluble fractions of cell lysates were obtained by centrifugation of lysates at 14,000 rpm for 10 min at 4 °C. Insoluble pellets were washed twice with lysis buffer and resuspended in 40 μl of lysis buffer. For whole cell lysates, cells were harvested and syringe-lysed in PBS plus a protease inhibitor tablet. Triton-soluble and -insoluble fractions were resolved by SDS-PAGE on a 7.5% gel, whereas whole cell lysates were resolved by SDS-PAGE on a 4–15% gradient gel (Bio-Rad). Following transfer to a nylon membrane (Millipore), blots were probed with either the Tau5 antibody (1:5,000; BD Biosciences), which recognizes an epitope in the polyproline region of Tau protein (intracellular transfected Tau) that is not present in the MTBR (extracellular Tau), or the GFP sc-8334 antibody (1:2,000; Santa Cruz Biotechnology). Blots were stripped and reprobed with the I-19-R anti-actin antibody (1:2,000; Santa Cruz Biotechnology). HA Y.11 (1:2,000, Covance) was used to probe for MTBR-HA Tau.

Immunofluorescence—All cells were grown on polyornithine-coated glass coverslips for microscopy. For visualization of intracellular Tau-YFP and MTBR-YFP, cells were transfected with Tau-YFP or MTBR-YFP. Cells were fixed with −20 °C methanol for 7 min and stained for α-tubulin (1:500; Sigma) followed by secondary staining with a rhodamine-conjugated anti-mouse antibody A546 (1:500; Molecular Probes). To visualize MTBR-AF488 aggregates inside cells, buffer, MTBR monomer, and MTBR aggregates were labeled with 62.5 ng/μl AF488 (Molecular Probes) for 1 h at room temperature and then overnight at 4 °C. Reactions were quenched with 100 mM glycine and added to cells. After 15 h, cells were treated with either PBS or 0.25% trypsin for 3 min and allowed to recover for 5 h before methanol fixation and staining for α-tubulin. Z-stacks were rendered into a three-dimensional image using the NIS-Elements AR 3.0 software (Nikon) from which an apical to distal slice containing the aggregate was obtained. For co-labeling with dextran, C17.2 cells were treated with MTBR-AF488 and 50 μg/ml rhodamine-dextran (M_r 10,000, pH neutral; Molecular Probes) for 4 h. Cells were trypsinized, fixed with 4% paraformaldehyde, and prepared as described above. For extracellular MTBR-HA and intracellular Tau-YFP co-localization studies, C17.2 cells expressing Tau-YFP were incubated with buffer, MTBR-HA monomer, or MTBR-HA aggregates for 15 h. Cells were trypsinized and allowed to recover as described before fixation with 4% paraformaldehyde. Cells were stained with the HA-Y11 antibody (1:1,000; Santa Cruz Biotechnology), followed by secondary labeling with rhodamine-conjugated anti-rabbit antibody (1:500; Molecular Probes). For co-culture experiments, C17.2 cells were transfected separately with MTBR-YFP and SV40-mCherry (a gift of Dr. Anthony Gerber) or Tau-YFP and mCherry. Cells were treated with Tau buffer, 0.4 μM Tau monomer, or 0.4 μM MTBR Tau aggregates. After the indicated co-culture incubation, cells were fixed for 7 min with 4% paraformaldehyde, stained with 4,6-diamidino-2-phenylindole (Sigma), and mounted on glass slides for imaging. Confocal microscopy was performed on a C1sl confocal microscope (Nikon Instruments Inc.).

Flow Cytometry—AF488 containing buffer or MTBR-AF488 was incubated with cells for the time indicated. Cells were harvested with 0.25% trypsin for 3 min and resuspended in PBS plus 10% fetal bovine serum prior to flow cytometry. Cells were counted in a FACSCalibur (BD Biosciences) flow cytometer. Each experiment was repeated four times, and 10,000 cells were counted in each individual experiment. For co-culture experiments, MTBR-YFP or Tau-YFP expressing cells were co-cultured with SV40-mCherry-expressing cells. Tau-YFP expressing cells were treated with buffer, MTBR monomer, or MTBR aggregates for indicated durations prior to flow cytometry. To collect dual positive cells, cells were sorted in a FACSAria cell sorter (BD Biosciences).

Sarkosyl Extraction—1% Sarkosyl-insoluble material was purified from cell lysates from a confluent 5-cm cell culture dish as described previously (20), with some modifications. Cell lysis buffer consisted of 10 mM Tris-HCl (pH 7.4), 0.8 M NaCl, 1 mM EGTA, 5 mM EDTA, 10% sucrose, and a protease inhibitor tablet (Roche Applied Science). Sarkosyl-insoluble pellets were resuspended in 50 μl of 10 mM HEPES and 100 mM NaCl (pH 7.4). When Sarkosyl-insoluble material from cells was used to seed the Tau monomer, the reactions contained 90 μl of 4 μM MTBR Tau monomer, 5 mM dithiothreitol, 100 mM NaCl, 10 mM HEPES, and 10 μl of syringe-sheared Sarkosyl-insoluble material from a 5-cm dish of buffer or MTBR aggregate-treated, Tau-YFP-expressing cells.

RESULTS

Full-length Tau Does Not Aggregate Spontaneously in Cells; Truncated Tau Forms Inclusions—To characterize the cellular activities of Tau, we used four different constructs (Fig. 1*A*). For expression in mammalian cells, we fused either full-length Tau (441 amino acids) or the microtubule-binding region (amino acids 243–375) to yellow fluorescent protein (YFP) (Tau-YFP and MTBR-YFP). For *in vitro* Tau fibrillization reactions, we created MTBR Tau with a hemagglutinin tag (MTBR-HA) and untagged MTBR. We expressed Tau-YFP in C17.2 neuronal precursor cells (21) by transient transfection. Tau-YFP co-localized with microtubules (Fig. 1, *B* and *F*), as others have reported (22, 23), and did not readily form inclusions. In contrast, MTBR-YFP did not bind microtubules and readily

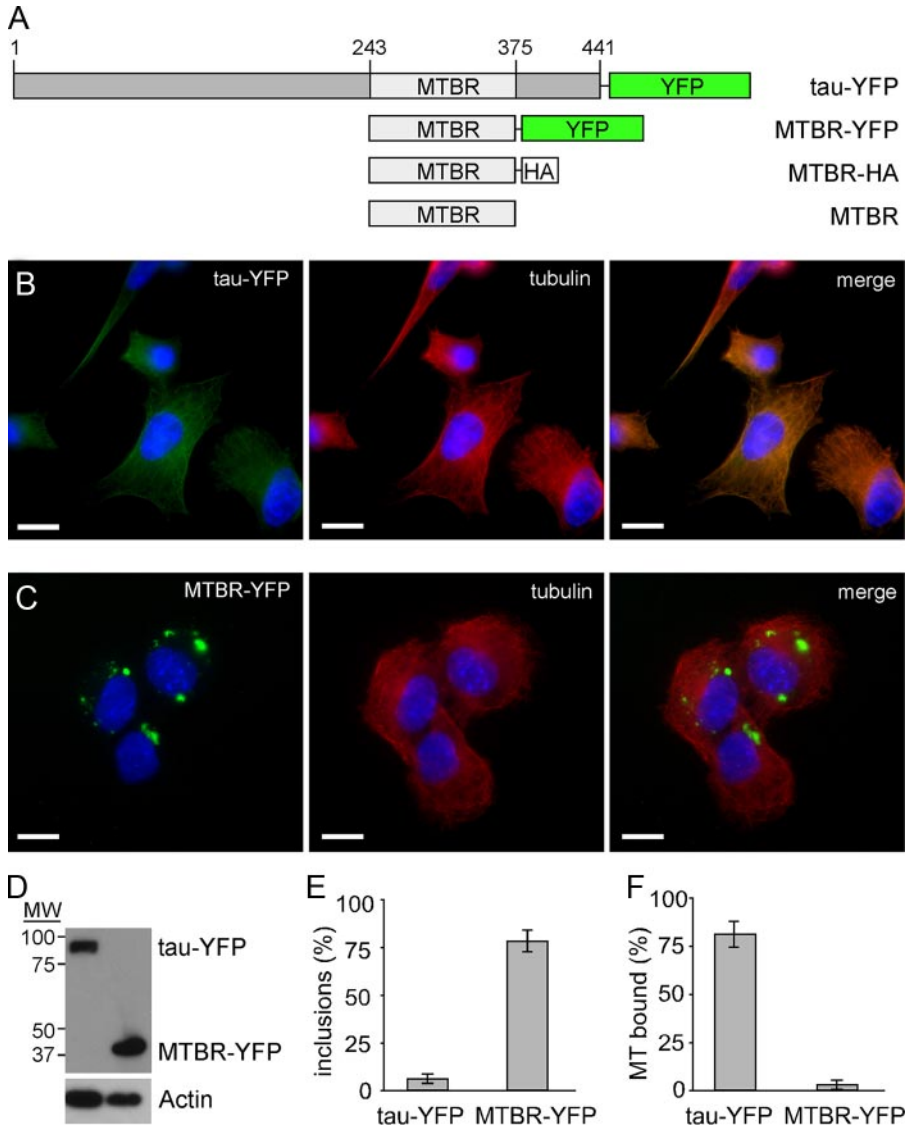

FIGURE 1. **Full-length Tau-YFP binds microtubules while MTBR-YFP aggregates in C17.2 neural cells.** *A,* Tau constructs. YFP fusion proteins were created for expression in mammalian cells as follows: full-length Tau (441 amino acids), Tau-YFP, the microtubule-binding region, MTBR-YFP. For bacterial expression, we used either MTBR alone or with a C-terminal hemagglutinin tag, MTBR-HA. *B,* Tau-YFP co-localizes with tubulin when transfected into C17.2 cells. *C,* MTBR-YFP does not co-localize with tubulin and spontaneously aggregates when transfected into C17.2 cells. *D,* Western blot showing similar expression levels of Tau-YFP and MTBR-YFP. Blots were probed with GFP and actin antibodies. *E,* based on counting transfected cells, 6% of cells have spontaneous aggregation of Tau-YFP, whereas 79% of cells have spontaneous aggregation of MTBR-YFP (n = 4, 100 transfected cells counted per experiment). *F,* 83% of cells have Tau-YFP that co-localizes with tubulin, whereas 3.5% of cells have MTBR-YFP that co-localizes with tubulin (n = 4, 100 transfected cells counted per experiment). *Scale bars,* 10 μm.

formed inclusions (Fig. 1, *C* and *E*) when expressed at a level comparable with Tau-YFP (Fig. 1*D*). 83% of cells expressing Tau-YFP exhibit co-localization with tubulin, whereas 3.5% of cells expressing MTBR-YFP exhibit co-localization with tubulin (Fig. 1*F*).

Tau Aggregates Enter C17.2 Cells—It has been shown previously that aggregated amyloid proteins amyloid β, prion protein, and expanded polyglutamine can gain entry into cells (24–27). Thus, we tested for uptake of recombinant Tau aggregates into C17.2 cells. First, we prepared recombinant MTBR-HA and used arachidonic acid to stimulate its fibrillization, which we detected using AFM (Fig. 2*A*). We found that these aggregates were completely digested when treated with 0.125% trypsin for 1 min (Fig. 2*B*). This is 50% of the level of trypsin used to re-plate cells in tissue culture (which are treated for 3 min), indicating relative sensitivity of the extracellular aggregates to proteolysis.

To determine whether Tau aggregates were taken into cells, we labeled MTBR Tau monomer and aggregates with AF488. We exposed C17.2 cells to AF488-containing buffer, AF488 conjugated to MTBR monomer, or MTBR aggregates. After 3 and 9 h, we harvested the cells from the plates by treating cells with 0.25% trypsin for 3 min. We quantified AF488 fluorescence using flow cytometry (Fig. 2*C*). Fluorescence signal due to background uptake of unconjugated AF488 in the buffer was subtracted from all samples. We observed significantly more uptake of aggregates compared with monomer at both time points (Fig. 2*C*). Direct visualization of these cells before and after trypsinization confirmed the conclusions derived from the flow cytometry experiment, indicating internalization of the aggregated species by the cells (Fig. 2, *D* and *E*). Aggregates of extracellularly derived Tau of various sizes were observed in cultured cells.

To verify that the Tau present after trypsinization was indeed intracellular, we stained MTBR-AF488 aggregate-treated cells for tubulin and visualized the cells using confocal microscopy. In cells that were treated with aggregates and imaged before trypsinization, both intracellular and extracellular membrane-associated aggregates were observed (data not shown). In trypsin-treated cells, however, the internalized aggregates displaced tubulin (Fig. 2*E*) and were present in the same plane as tubulin (Fig. 2*E, bar*), confirming their intracellular locale.

Tau Aggregates Enter C17.2 Cells and Co-localize with Dextran—It has been shown previously that exogenously derived amyloid β and prion protein aggregates co-localize with dextran, a marker of fluid-phase endocytosis. Such aggregates did not co-localize with cholera toxin subunit B, a marker of lipid rafts (26). We exposed C17.2 cells to MTBR-AF488 Tau aggregates and dextran. 24% of Tau aggregates co-localized with dextran (n = 3, 200 aggregates counted per experiment) (Fig. 3) but did not co-localize with cholera toxin B (data not

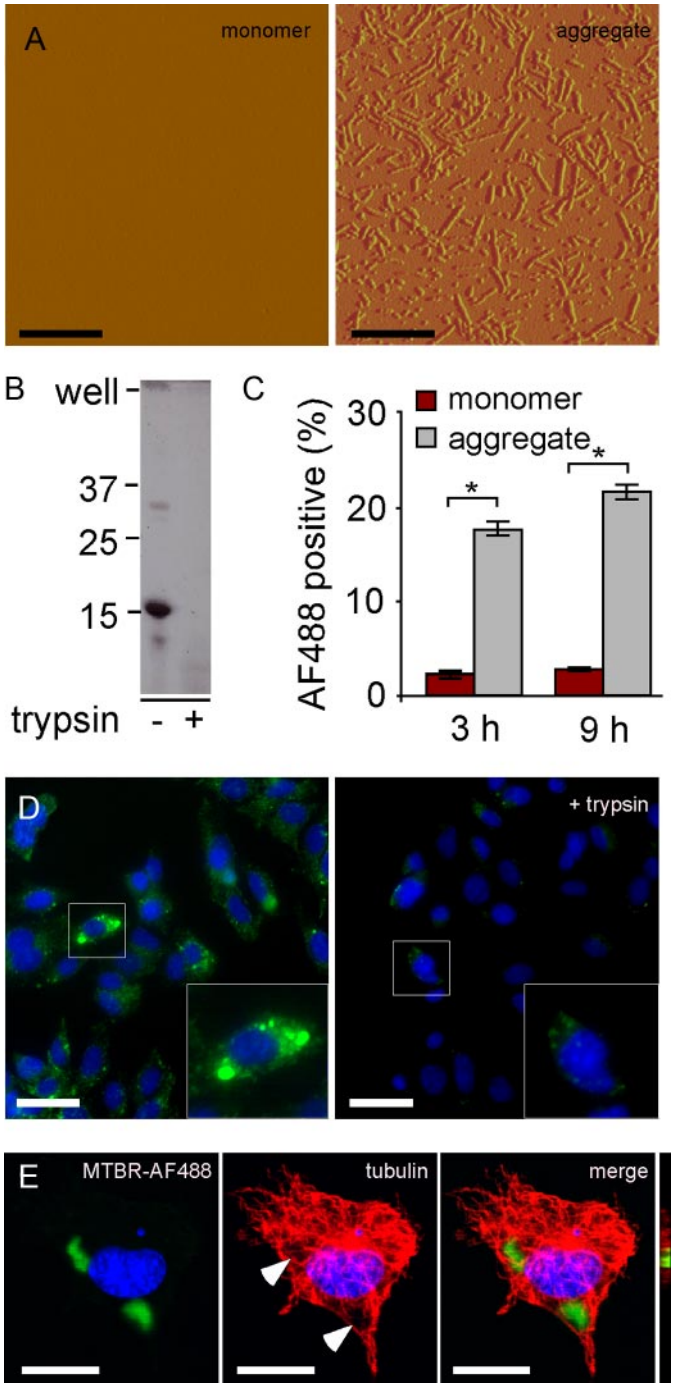

FIGURE 2. **C17.2 cells take up aggregated Tau.** *A,* recombinant MTBR Tau was prepared *in vitro* and induced to fibrillize using arachidonic acid. Tau monomer is not detectable via AFM. After 24 h of incubation with arachidonic acid, however, Tau is highly aggregated, forming many oligomeric and fibrillar species. *Scale bars,* 600 nm. *B,* aggregated Tau was treated with buffer or 0.125% trypsin for 1 min and resolved by SDS-PAGE 4–15% gradient gel, followed by Coomassie stain. Aggregated Tau is very sensitive to trypsin digestion. *C,* C17.2 cells were exposed to AF488-containing buffer, AF488-labeled monomer, or aggregates. After 3 and 9 h, cells were harvested by 0.25% trypsin treatment. Intracellular AF488 fluorescence was then quantified by flow cytometry. After 3 h, 2.0% of monomer-treated cells scored positive, *versus* 18% for aggregate-treated cells. After 9 h, 3.0% of monomer-treated cells scored positive, *versus* 22% for aggregate-treated cells. *, $p < 10^{-6}$ (unpaired *t* test, $n = 4$, 10,000 cells counted per experiment). *D,* MTBR-AF488 aggregate-treated C17.2 cells with or without trypsin treatment and visualized by confocal microscopy. *Scale bar,* 30 μm. *E,* MTBR-AF488 aggregate-treated C17.2 cell stained for tubulin and visualized via confocal microscopy after treatment with 0.25% trypsin illustrates internalized aggregates.

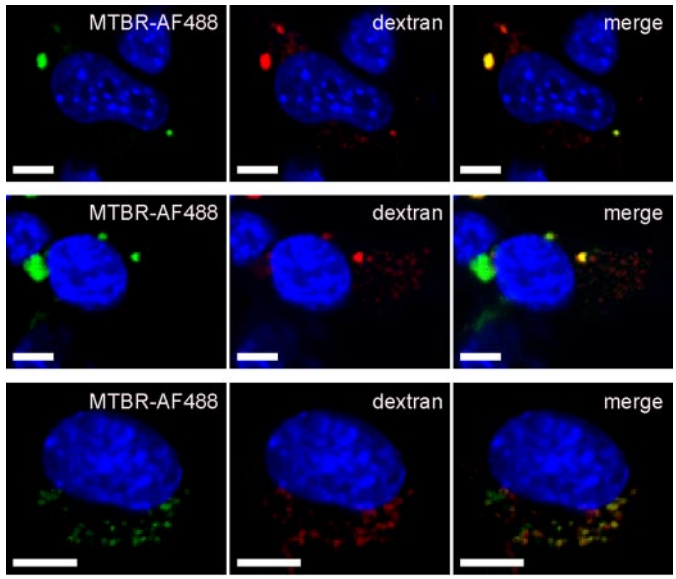

FIGURE 3. **Multiple images of C17.2 cells treated with MTBR-AF488 aggregates and rhodamine-dextran contain co-localizing and non-co-localizing aggregates.** *Scale bars,* 5 μm.

shown). This suggests that Tau aggregates enter cells via an endocytic pathway involving engulfment by the cell membrane, rather that the simple penetration of the membrane, as has been proposed previously for other amyloid-forming proteins (28).

Exogenous Tau Aggregates Induce Aggregation of Intracellular Full-length Tau-YFP—Tau fibrils propagate *in vitro* via seeded polymerization (29). We thus tested whether extracellular Tau aggregates that enter cells would trigger the misfolding of intracellular Tau-YFP. We transiently transfected HEK293 cells with Tau-YFP. We treated these cells with buffer, MTBR monomer, or MTBR aggregates. After 15 h, cells were harvested and lysed in 1% Triton, and extracts were fractionated by centrifugation at 15,000 × *g*. After SDS-PAGE, Western blot was performed using the Tau5 antibody, which recognizes a motif in the polyproline region of full-length Tau that is not present in the MTBR. Cells treated with aggregates, but not buffer or monomer, contained detergent-insoluble Tau-YFP (Fig. 4*A*). We repeated this experiment in C17.2 neural cells, including a negative control in which we mixed MTBR aggregates with cell lysate containing Tau-YFP prior to SDS-PAGE to rule out induction of aggregation following lysis (Fig. 4*B*). To confirm Tau-YFP aggregation in C17.2 cells, detergent-free whole cell lysates were created and resolved by Western blot with the Tau5 antibody. We observed Tau-YFP aggregates at the top of the well when cells were treated with MTBR aggregates but not after buffer or monomer exposure (Fig. 4*C*). To determine the specificity of aggregate induction, we treated Tau-YFP-expressing cells with aggregates of Huntingtin exon 1 containing 53 glutamines. Exogenous aggregated Huntingtin had no effect on intracellular Tau-YFP aggregation based on Western blot (data not shown).

Arrows indicate displacement of tubulin. An apical-to-distal slice (*bar*) obtained from a three-dimensional image rendered from Z-stacks shows MTBR-AF488 in the same plane as tubulin. *Scale bar,* 10 μm.

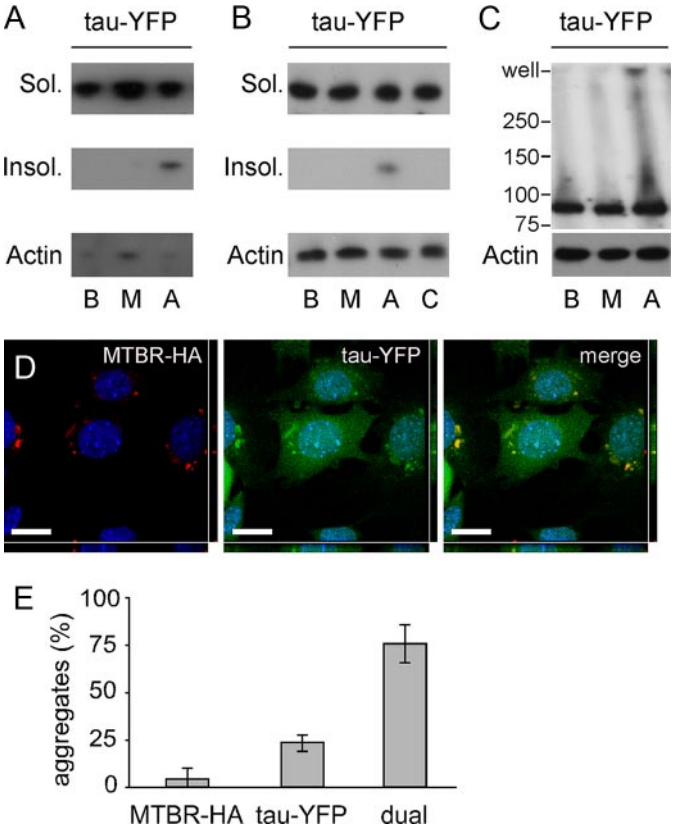

FIGURE 4. **Extracellular Tau enters cells and induces aggregation of full-length Tau-YFP in HEK293 and C17. 2 cells.** HEK293 cells (*A*) or C17.2 cells (*B*) expressing Tau-YFP were treated for 15 h with buffer (*lane B*), MTBR monomer (*lane M*), or MTBR aggregates (*lane A*) followed by 1% Triton detergent fractionation. Control cells (*lane C*) were lysed and treated with aggregates. Soluble (*Sol.*) and insoluble (*Insol.*) Tau-YFP bands were detected using the Tau5 antibody, with actin as a loading control. Treatment with Tau aggregates increased insoluble Tau-YFP in both cell types. *C,* C17.2 cells expressing Tau-YFP were treated for 15 h with buffer, MTBR monomer, or MTBR aggregates, followed by syringe lysis in PBS. The whole cell lysate was loaded onto a 4–15% SDS-polyacrylamide gel, and blotted with a GFP antibody or an actin antibody to control for loading. Full-length aggregated Tau-YFP appears in the well when cells are treated with MTBR aggregates. *D,* C17.2 cells expressing Tau-YFP were exposed to MTBR-HA aggregates, and double label confocal microscopy was performed using an HA antibody (*red channel*) and direct visualization of YFP (*green channel*). A representative example of co-localization between MTBR-HA (exogenous) and Tau-YFP (endogenous) aggregates is shown. *Scale bar* = 10 μm. *E,* 3% of aggregates were composed of MTBR-HA in the absence of Tau-YFP aggregates; 23% of aggregates were composed of Tau-YFP in the absence of MTBR-HA aggregates; 74% of aggregates were dual-fluorescent, composed of Tau-YFP and MTBR-HA (n = 3, 100 aggregates counted per experiment).

Taken together, these experiments indicated that extracellular Tau aggregates enter cells and induce misfolding of intracellular Tau, but left uncertain whether this was because of a direct association of exogenous and endogenous protein. Thus, we used double label fluorescence confocal microscopy to test for co-localization of exogenous MTBR-HA and endogenous Tau-YFP. After treatment with MTBR-HA aggregates for 15 h and visualization via confocal microscopy, we observed intracellular inclusions consisting of both exogenously and endogenously derived protein, most of which co-localized (Fig. 4*D*). 74% of aggregates observed were composed of both MTBR-HA and Tau-YFP; 23% of aggregates were composed only of Tau-YFP; and 3% of aggregates were composed only of MTBR-HA (Fig. 4*E*). Tau-YFP aggregates observed in the absence of MTBR-HA co-localization may arise from self-seeding or may contain MTBR-HA seeds that are too small to detect via immunofluorescence.

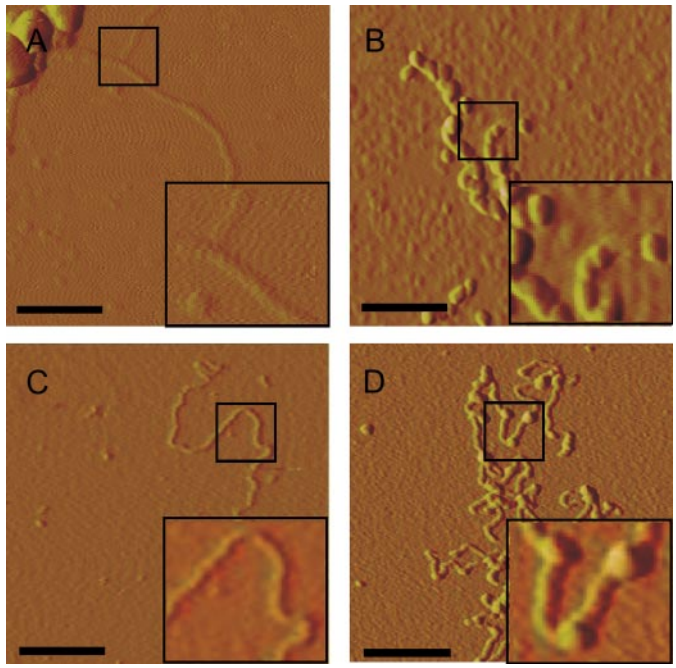

FIGURE 5. **Induced Tau-YFP aggregates in C17.2 cells are fibrillar and seed MTBR fibrillization *in vitro*.** C17.2 cells, in which Tau-YFP aggregation was induced by treatment with MTBR aggregates, were extracted with Sarkosyl. *Scale bars,* 0.2 μm. *A,* insoluble material was visualized by AFM, which demonstrates fibrils. *B,* Tau5 antibody labeling increases the diameter of the observed fibrils, indicating their principle constituent is Tau-YFP. *C,* Sarkosyl-extracted Tau-YFP fibrils from aggregate-treated cells were used to seed the fibrillization of recombinant MTBR *in vitro*. The resultant fibrils were visualized by AFM. *D,* MTBR fibrils seeded by Tau-YFP were exposed to Tau5 antibody, which labels the Tau-YFP seeds within the MTBR fibrils.

Extracellular Tau Aggregates Induce Fibrillization of Intracellular Tau-YFP—To rule out the possibility that exogenously derived aggregated Tau caused disordered aggregation of intracellular Tau-YFP, rather than fibrillization, we purified induced Tau-YFP aggregates from cells. We treated C17.2 cells expressing Tau-YFP with buffer or aggregates, and we examined the Sarkosyl-insoluble fraction (20) from cell lysates using AFM. No fibrillar material was observed except in cells exposed to exogenous MTBR Tau aggregates (Fig. 5*A*). To confirm that these fibrils were derived from intracellular full-length Tau-YFP, and not the exogenous MTBR Tau aggregates or other proteins, we used antibody decoration (30) with the Tau5 antibody. We observed an increase in fibril diameter along the length of the fibrils in Tau5-treated extracts, indicating the purified fibrils were composed of Tau-YFP (Fig. 5*B*). We next used Sarkosyl-insoluble Tau-YFP purified from C17.2 cells to seed the fibrillization of recombinant MTBR *in vitro*, confirming the conversion of Tau-YFP to a fibrillar form that is competent to seed aggregation of Tau monomer (Fig. 5*C*). Antibody decoration of the seeded fibrils using the Tau5 antibody produced isolated densities on the fibrils, confirming the source of the seed as Tau-YFP (Fig. 5*D*). Thus, exposure to exogenous Tau aggregates induces intracellular Tau-YFP to form fibrils that are competent to seed further aggregation.

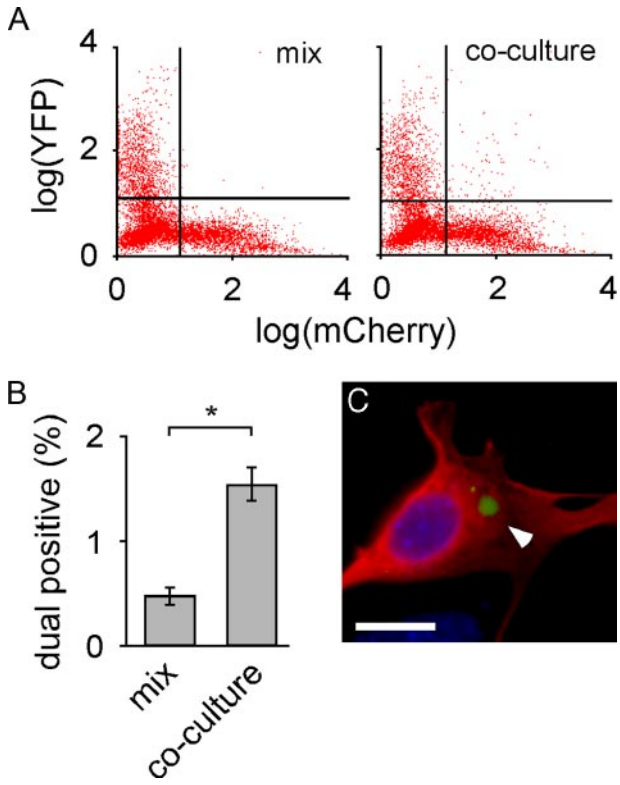

FIGURE 6. **MTBR-YFP aggregates transfer between co-cultured cells.** *A,* cells were transfected separately with mCherry or MTBR-YFP. The two cell populations were either mixed immediately prior to analysis or co-cultured for 24 h. Flow cytometry was used to quantify dual positive cells (10,000 cells sorted per condition). *B,* quantification of flow cytometry revealed that 0.5% of cells scored positive for mCherry and YFP (*upper right quadrant* of cell plot) when cells were simply mixed prior to sorting, *versus* 1.5% of cells that scored dual positive when cells were co-cultured for 24 h, indicating transfer of MTBR-YFP between cells. *, $p < 10^{-5}$ (unpaired *t* test, $n = 4$, 10,000 cells sorted per experiment). *C,* dual positive cells were collected via FACS, fixed, and mounted. A MTBR-YFP inclusion (*white arrowhead*) is visible within an mCherry-expressing cell. *Scale bar,* 10 μm.

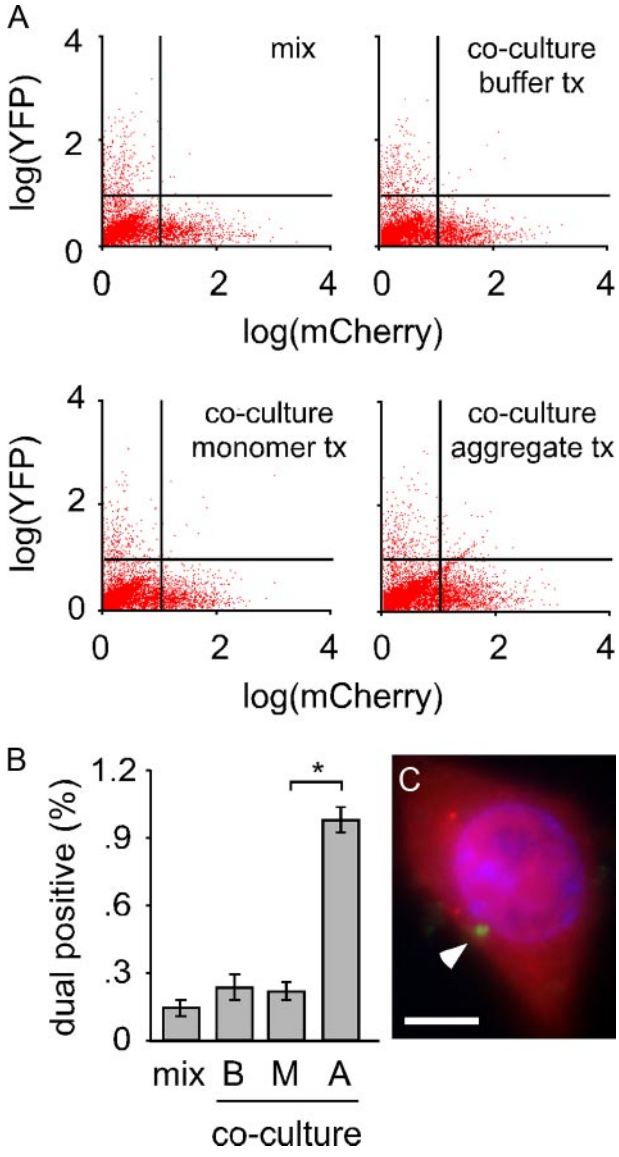

FIGURE 7. **Tau-YFP aggregates transfer between co-cultured cells.** *A,* cells were transfected separately with mCherry or Tau-YFP. The two cell populations were either mixed immediately prior to analysis or co-cultured for 48 h. Co-cultured cells were treated with buffer, monomer, or aggregates, followed by flow cytometry (10,000 cells sorted per condition). *tx,* treatment. *B,* quantification of flow cytometry revealed that 0.15% of cells score positive for mCherry and YFP (*upper right quadrant* of cell plot) when cells were mixed immediately prior to counting. 0.3 and 0.25% of cells are dual positive when cells are treated with buffer (*B*) or monomer (*M*), *versus* 1% when treated with Tau aggregates (*A*), indicating transfer of aggregated full-length Tau-YFP between cells. *, $p < 10^{-7}$ (unpaired Student's *t* test, $n = 4$, 10,000 cells counted per experiment). *C,* dual positive cells were collected, fixed, and mounted. Direct visualization indicates a Tau-YFP inclusion (*white arrowhead*) within an mCherry-expressing cell. *Scale bar,* 10 μm.

Intracellular Tau-YFP Aggregates Transfer between Co-cultured Cells—We next tested whether intracellular Tau aggregates transfer between co-cultured cells. We separately transfected cells with either MTBR-YFP or mCherry (a red fluorescent protein variant) and then co-cultured them for 24 h. As a control, we cultured MTBR-YFP and mCherry cells separately and mixed them immediately prior to flow cytometry. Co-cultured cells had significantly more YFP/mCherry dual positive cells (Fig. 6*A*). Based on four independent experiments, 0.48% of mixed cells (*i.e.* background) scored as dual-fluorescent *versus* 1.6% of co-cultured cells (Fig. 6*B*). Dual positive cells were collected and viewed via fluorescence microscopy. This confirmed the presence of MTBR-YFP inclusions inside cells expressing mCherry (Fig. 6*C*), indicating that transfer of MTBR-YFP aggregates had occurred. To determine whether the transfer of Tau aggregates between co-cultured cells is inducible, we co-cultured cells expressing full-length Tau-YFP and mCherry and initiated misfolding of Tau-YFP by exposing cells to MTBR Tau aggregates for 48 h (Fig. 7*A*). Treatment with aggregated species caused Tau-YFP aggregation and transfer of these species to 1% of the mCherry cells (Fig. 7*B*). We sorted dual positive cells and imaged them with fluorescence microscopy. This confirmed the presence of Tau-YFP inclusions in mCherry-expressing cells (Fig. 7*C*). Simple cell fusion was unlikely to have occurred at a significant rate, because buffer and monomer treated cells did not score positive. Thus, spontaneously formed MTBR-YFP Tau intracellular inclusions or induced full-length Tau-YFP inclusions spontaneously transfer between co-cultured cells.

DISCUSSION

We have tested the hypothesis that aggregated extracellular Tau enters cells and transmits a misfolded state specifically to intracellular Tau. We used recombinant MTBR Tau prepared *in vitro* to form aggregates, which were readily taken up by

cultured cells. Full-length Tau-YFP protein does not readily aggregate within the cell, but internalized aggregates induce its fibrillization. When purified from cells, Tau-YFP is competent to seed the fibrillization of Tau monomer *in vitro*. Finally, we observed that aggregated intracellular Tau transfers between co-cultured cells. We are uncertain how an aggregate taken into an endocytic vesicle might ultimately gain access to protein located in the cytoplasm, and whether aggregates that transfer from one cell to another are capable of inducing further intracellular aggregation. Aggregate uptake and induced aggregation in neighboring cells was recently suggested by co-culture of polyglutamine-expressing cells, although this study failed to document direct transfer of aggregated protein (27). Relatively low efficiencies of cell-to-cell aggregate transfer and extracellular-to-intracellular seeding may make it difficult to document these events *in vitro*.

It is unknown why misfolded amyloid protein accumulates progressively throughout the brain in tauopathy and other neurodegenerative diseases. These data provide a plausible cellular mechanism and are consistent with the hypothesis that Tau aggregates propagate protein misfolding within the brain. Such aggregates could be released from dead or dying cells. Alternatively, they might move between cells via an exocytic process, as has been suggested for prion protein (31). Following uptake by healthy neurons, the aggregates might stimulate further misfolding of an otherwise stable intracellular protein, in the manner of prions. The exocytosis model is more consistent with the observation that spread of Tau pathology traditionally affects networks of neurons that are synaptically connected (8), although both mechanisms could act in concert to transfer Tau aggregates between cells. These ideas await testing *in vivo*. We predict that introduction of exogenous fibrillar protein into the brain of a susceptible animal, like prions, will induce further aggregation of endogenous protein and progressive pathology.

We have recently shown that wild-type Tau is capable of conformational diversity that depends on templated conformation change (32). These data, along with our present study, suggest a mechanism to explain disease-specific cellular vulnerabilities to misfolded protein based on fibrillization rate and propensity for propagation of a given misfolded species. Indeed, splicing variants or post-translational modifications of Tau (*e.g.* phosphorylation) could render a subgroup of neurons particularly vulnerable to spontaneous or seeded protein misfolding. Thus the propagation of misfolded species through the brain would reflect a combination of neuronal proximity, connectivity, and the particular Tau moieties expressed within the involved regions. Finally, propagation via progressive, templated misfolding suggests a general pathogenic mechanism for other neurodegenerative diseases linked to amyloid protein aggregation.

Acknowledgments—We thank Jonathan Weissman for use of the atomic force microscope. We thank the Nikon Imaging Center and Kurt Thorn, University of California, San Francisco, for use of the Nikon C1sl spectral confocal microscope. Sara Elmes provided technical expertise with fluorescence-activated cell sorting. Tony Gerber provided the mCherry vector. Virginia Lee provided the vector from which constructs were subcloned.

REFERENCES

1. Lee, V. M., Goedert, M., and Trojanowski, J. Q. (2001) *Annu. Rev. Neurosci.* **24,** 1121–1159
2. Hutton, M., Lendon, C. L., Rizzu, P., Baker, M., Froelich, S., Houlden, H., Pickering-Brown, S., Chakraverty, S., Isaacs, A., Grover, A., Hackett, J., Adamson, J., Lincoln, S., Dickson, D., Davies, P., Petersen, R. C., Stevens, M., de Graaff, E., Wauters, E., van Baren, J., Hillebrand, M., Joosse, M., Kwon, J. M., Nowotny, P., Che, L. K., Norton, J., Morris, J. C., Reed, L. A., Trojanowski, J., Basun, H., Lannfelt, L., Neystat, M., Fahn, S., Dark, F., Tannenberg, T., Dodd, P. R., Hayward, N., Kwok, J. B., Schofield, P. R., Andreadis, A., Snowden, J., Craufurd, D., Neary, D., Owen, F., Oostra, B. A., Hardy, J., Goate, A., van Swieten, J., Mann, D., Lynch, T., and Heutink, P. (1998) *Nature* **393,** 702–705
3. Poorkaj, P., Bird, T. D., Wijsman, E., Nemens, E., Garruto, R. M., Anderson, L., Andreadis, A., Wiederholt, W. C., Raskind, M., and Schellenberg, G. D. (1998) *Ann. Neurol.* **43,** 815–825
4. Spillantini, M. G., Murrell, J. R., Goedert, M., Farlow, M. R., Klug, A., and Ghetti, B. (1998) *Proc. Natl. Acad. Sci. U. S. A.* **95,** 7737–7741
5. Liu, W., Miller, B. L., Kramer, J. H., Rankin, K., Wyss-Coray, C., Gearhart, R., Phengrasamy, L., Weiner, M., and Rosen, H. J. (2004) *Neurology* **62,** 742–748
6. Braak, H., and Braak, E. (1991) *Acta Neuropathol.* **82,** 239–259
7. Braak, H., and Braak, E. (1997) *Neurobiol. Aging* **18,** 351–357
8. Delacourte, A., David, J. P., Sergeant, N., Buee, L., Wattez, A., Vermersch, P., Ghozali, F., Fallet-Bianco, C., Pasquier, F., Lebert, F., Petit, H., and Di Menza, C. (1999) *Neurology* **52,** 1158–1165
9. Arnold, S. E., Hyman, B. T., Flory, J., Damasio, A. R., and Van Hoesen, G. W. (1991) *Cereb. Cortex* **1,** 103–116
10. Sergeant, N., Wattez, A., and Delacourte, A. (1999) *J. Neurochem.* **72,** 1243–1249
11. Akiyama, H., Barger, S., Barnum, S., Bradt, B., Bauer, J., Cole, G. M., Cooper, N. R., Eikelenboom, P., Emmerling, M., Fiebich, B. L., Finch, C. E., Frautschy, S., Griffin, W. S., Hampel, H., Hull, M., Landreth, G., Lue, L., Mrak, R., Mackenzie, I. R., McGeer, P. L., O'Banion, M. K., Pachter, J., Pasinetti, G., Plata-Salaman, C., Rogers, J., Rydel, R., Shen, Y., Streit, W., Strohmeyer, R., Tooyoma, I., Van Muiswinkel, F. L., Veerhuis, R., Walker, D., Webster, S., Wegrzyniak, B., Wenk, G., and Wyss-Coray, T. (2000) *Neurobiol. Aging* **21,** 383–421
12. Delacourte, A. (2005) *Polish Acad. Sci.* **43,** 244–257
13. Gomez-Ramos, A., Diaz-Hernandez, M., Cuadros, R., Hernandez, F., and Avila, J. (2006) *FEBS Lett.* **580,** 4842–4850
14. Gomez-Ramos, A., Diaz-Hernandez, M., Rubio, A., Miras-Portugal, M. T., and Avila, J. (2008) *Mol. Cell. Neurosci.* **37,** 673–681
15. Asuni, A. A., Boutajangout, A., Quartermain, D., and Sigurdsson, E. M. (2007) *J. Neurosci.* **27,** 9115–9129
16. Weingarten, M. D., Lockwood, A. H., Hwo, S. Y., and Kirschner, M. W. (1975) *Proc. Natl. Acad. Sci. U. S. A.* **72,** 1858–1862
17. Vandermeeren, M., Mercken, M., Vanmechelen, E., Six, J., van de Voorde, A., Martin, J. J., and Cras, P. (1993) *J. Neurochem.* **61,** 1828–1834
18. Endoh, R., Ogawara, M., Iwatsubo, T., Nakano, I., and Mori, H. (1993) *Brain Res.* **601,** 164–172
19. Goedert, M., and Jakes, R. (1990) *EMBO J.* **9,** 4225–4230
20. Greenberg, S. G., and Davies, P. (1990) *Proc. Natl. Acad. Sci. U. S. A.* **87,** 5827–5831
21. Ryder, E. F., Snyder, E. Y., and Cepko, C. L. (1990) *J. Neurobiol.* **21,** 356–375
22. Trinczek, B., Biernat, J., Baumann, K., Mandelkow, E. M., and Mandelkow, E. (1995) *Mol. Biol. Cell* **6,** 1887–1902
23. King, M. E., Kan, H. M., Baas, P. W., Erisir, A., Glabe, C. G., and Bloom, G. S. (2006) *J. Cell Biol.* **175,** 541–546
24. Kanu, N., Imokawa, Y., Drechsel, D. N., Williamson, R. A., Birkett, C. R., Bostock, C. J., and Brockes, J. P. (2002) *Curr. Biol.* **12,** 523–530
25. Yang, W., Dunlap, J. R., Andrews, R. B., and Wetzel, R. (2002) *Hum. Mol. Genet.* **11,** 2905–2917
26. Magalhaes, A. C., Baron, G. S., Lee, K. S., Steele-Mortimer, O., Dorward, D., Prado, M. A., and Caughey, B. (2005) *J. Neurosci.* **25,** 5207–5216

27. Ren, P. H., Lauckner, J. E., Kachirskaia, I., Heuser, J. E., Melki, R., and Kopito, R. R. (2009) *Nat. Cell Biol.* **11,** 219–225
28. Kayed, R., Sokolov, Y., Edmonds, B., McIntire, T. M., Milton, S. C., Hall, J. E., and Glabe, C. G. (2004) *J. Biol. Chem.* **279,** 46363–46366
29. Friedhoff, P., von Bergen, M., Mandelkow, E. M., Davies, P., and Mandelkow, E. (1998) *Proc. Natl. Acad. Sci. U. S. A.* **95,** 15712–15717
30. DePace, A. H., and Weissman, J. S. (2002) *Nat. Struct. Biol.* **9,** 389–396
31. Fevrier, B., Vilette, D., Archer, F., Loew, D., Faigle, W., Vidal, M., Laude, H., and Raposo, G. (2004) *Proc. Natl. Acad. Sci. U. S. A.* **101,** 9683–9688
32. Frost, B., Ollesch, J., Wille, H., and Diamond, M. I. (2009) *J. Biol. Chem.* **284,** 3546–3551